

# Conformation of oligo(ethylene glycol) grafted polystyrene in dilute aqueous solutions

Gang Cheng<sup>a</sup>, Yuri B. Melnichenko<sup>a,\*\*</sup>, George D. Wignall<sup>a</sup>, Fengjun Hua<sup>b</sup>,  
Kunlun Hong<sup>b,\*</sup>, Jimmy W. Mays<sup>b</sup>

<sup>a</sup> Neutron Scattering Sciences Division, Oak Ridge National Laboratory, Oak Ridge, TN 37831, United States

<sup>b</sup> Chemical Science Division and Center for Nanophase Materials Sciences, Oak Ridge National Laboratory, Oak Ridge, TN 37831, United States

Received 3 January 2007; received in revised form 9 May 2007; accepted 10 May 2007

Available online 18 May 2007

## Abstract

Temperature induced conformational changes of poly(*p*-oligo(ethylene glycol) styrene) (POEGS) in aqueous solutions were investigated by small angle neutron scattering (SANS), neutron transmission and dynamic light scattering (DLS). The molecular weight of the polymer studied was 9400 g/mol with a polydispersity index of 1.18 and each repeat unit of the polymer had four ethylene glycol monomer segments. The polymer was water soluble due to the hydrophilicity of the OEG side chains and these solutions showed lower critical solution temperature (LCST) depending on the concentration of the polymer. Measurements of solution behavior were made as a function of temperature in the range of 25–55 °C for three polymer concentrations (0.1 wt%, 0.3 wt%, and 1.8 wt%). Neutron transmission measurements were used to monitor the amount of polymer which precipitated or remained in solution above the cloud point temperature ( $T_{CP}$ ). DLS revealed the presence of large clusters in all solutions both below and above  $T_{CP}$  while SANS provided information on the structure and interactions between individual chains. It was found that in the homogeneous region below  $T_{CP}$  the shape of individual polymers in solution was close to ellipsoidal with the dimensions  $R_a = 37 \text{ \AA}$  and  $R_b = 14 \text{ \AA}$  and was virtually independent of temperature. The SANS data taken for the most concentrated solution studied (1.8 wt%) were fit to the ellipsoidal model with attractive interactions which were approximated by the Ornstein–Zernike function with a temperature-dependent correlation length in the range of 24–49 Å. The collapse of individual polymers to spherical globules with the radius of 15 Å above  $T_{CP}$  was observed.

© 2007 Elsevier Ltd. All rights reserved.

**Keywords:** SANS; Thermo-sensitive polymers; Conformation

## 1. Introduction

Water-soluble polymers exhibiting structural and property changes in response to temperature have received a great deal of attention in biomedical applications [1], microfluidic (microchemical) systems [2], catalysis [3], and environmentally responsive emulsions [4]. Understanding the fundamentals of the conformational changes during the phase transition is imperative for these applications. An extensively

studied system showing such behaviors is poly(*N*-isopropylacrylamide) (PNIPAM), which exhibits a lower critical solution temperature (LCST) of  $\sim 34 \text{ °C}$  [5–9]. In dilute solution the coil-to-globule transition of this polymer near the LCST has been observed by light scattering; and the transition is accompanied by partial dehydration and intra-molecular contraction [6]. A recent dielectric study suggests that PNIPAM possesses 11 water molecules per monomer unit in homogeneous aqueous solution and completely dehydrates near the LCST [8]. In addition to PNIPAM, poly(ethylene glycol) (PEG) and PEG-containing polymers have also been investigated extensively due to the unique properties of PEG, including nontoxicity, ion-transporting ability, nonrecognition by the human immune system, etc. In many cases, branched PEGs are preferred over

\* Corresponding author. Tel.: +1 865 574 4974; fax: +1 865 574 1753.

\*\* Corresponding author. Tel.: +1 865 576 7746.

E-mail addresses: [melnichenko@ornl.gov](mailto:melnichenko@ornl.gov) (Y.B. Melnichenko), [hongkq@ornl.gov](mailto:hongkq@ornl.gov) (K. Hong).

linear PEG chains due to crystallization difference. To this end, star-like, comb-like and dendrimer-like PEGs have been synthesized [10]. PEG-grafted comb polymers, in particular, have found many uses including applications in solid phase ionic conductors [11], compatibilizers in polymer blends [12], catalysts for phase transfer reactions [13], colloidal stabilizers [14], and in modifying surfaces to prevent nonspecific protein or bacterial adhesion [15].

Despite numerous studies of comb-like PEG-grafted polymers, some fundamental issues such as conformation and phase behavior in water have not attracted much attention [16]. On the molecular level, these “hairy” or comb-like copolymers consist of a backbone chain with multiple trifunctional branch points from each of which a linear side chain emanates. Their conformation is affected by many factors such as the number of side chains per unit monomer, molecular weight of the backbone and side chain, and solvent quality [18,19]. When both the side chains and backbone are sufficiently long, the polymers can be highly extended to give a “topological” stiffness [17], and have been described as a “molecular bottle-brush” [18]. However, when the backbone is placed in a poor solvent, the intra-molecular attraction will influence the overall conformation [19,20].

SANS is a powerful technique to study solution properties of polymers on length scales in the order of 10–1000 Å. It has been used to investigate thermoresponsive polymers, such as PNIPAM [7,21,22]. Previously, we have reported the synthesis of poly(*p*-oligo(ethylene glycol) styrene)s by nitroxide-mediated radical polymerization which were found to exhibit LCSTs in water [23]. Each styrenic monomer bears one side chain consisting of four EG monomers end-capped with a methyl group. In this article, we report results of combined DLS and SANS studies of the structure of dilute poly(*p*-tetraakis(ethylene glycol) styrene) (PTrEGS) solutions in D<sub>2</sub>O as a function of temperature and concentration. The neutron transmission data are used to evaluate the amount of polymer that remains in the solution above  $T_{CP}$ . DLS provides data on the size of the large polymer clusters in solutions at different temperatures. SANS gives information on conformation and interactions between individual polymers both below and above  $T_{CP}$  [24].

## 2. Experimental section

### 2.1. Materials

The chemical structure of the monomer is shown in the inset of Fig. 1. The weight-average molecular weight,  $M_w$ , of the polymer is 9400 g/mol and the polydispersity index is 1.18, as determined by gel permeation chromatography. The densities of the backbone and side chains are assumed to be that of PS (1.05 g/cm<sup>3</sup>) and PEG (1.12 g/cm<sup>3</sup>), respectively. The dry volume of one polymer molecule is calculated from the density and molecular weight as  $V_p = 14\,300 \text{ \AA}^3$ .

Cloud points were measured by placing the solutions in the water bath (Neslab RTE 7 refrigerated circulator) which was controlled to be within  $\pm 0.1 \text{ }^\circ\text{C}$ . The temperature was

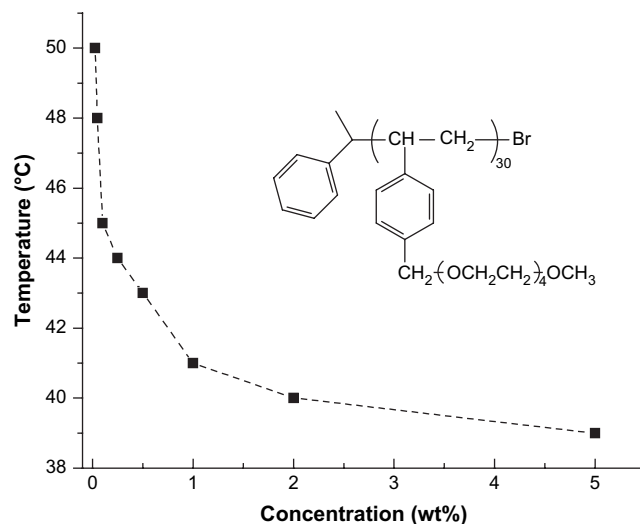


Fig. 1. Cloud point temperature curve of aqueous solutions of PTrEGS in H<sub>2</sub>O. Inset is the chemical structure of the polymer.

increased in steps of 1 °C and it was found that the solutions reach equilibrium at a new temperature after 5 min. The  $T_{CP}$  was recorded when the polymer solution became opaque. The  $T_{CPs}$  of the PTrEGS solutions in D<sub>2</sub>O as a function of concentration are shown in Fig. 1.

### 2.2. Dynamic light scattering (DLS)

DLS measurements were conducted with a PDE Expert (Multi Angle Light Scattering Platform) equipped with a Precision Detector, digital correlator, a temperature controller, and a solid-state laser (model 25-LHP-928-249,  $\lambda = 823 \text{ nm}$ ) at a scattering angle of 90°. The copolymers were dissolved in deionized water or deuterated water in an ice/water bath at 5 °C and the clear solutions were filtered into borosilicate glass tubes with an inner diameter of 4 mm by use of Millipore Teflon filters (800 nm pore size). The tubes were then sealed and were thermostated in a sample vat connected to a refrigerated circulator (Fisher Scientific) for 24 h before the measurements. The data were recorded at each temperature after the solutions were equilibrated for 20 min. The second-order correlation function of the scattered light intensity,  $g^{(2)}(t)$ , was analyzed by the CONTIN analysis method.  $g^{(2)}(t)$  can be expressed by the following equation:

$$|g^{(2)}(t)| = A \left( 1 + \beta |g^{(1)}(t)|^2 \right)$$

where  $A$  is the baseline,  $\beta$  is the coherence factor determined by the geometry of the detection, and  $g^{(1)}(t)$  is the normalized electric field correlation function. Generally,  $g^{(1)}(t)$  is expressed by the distribution function  $G(\Gamma)$  of the decay time  $\tau$  as:

$$|g^{(1)}(t)| = \int G(\Gamma) \exp(-\Gamma t) d\Gamma$$

For a translational diffusion mode,  $\Gamma$  can be used to determine the diffusion coefficient  $D$  through  $\Gamma = Dq^2$ , where  $q$  is the

scattering vector. The hydrodynamic radius  $R_h$  is related to the diffusion coefficient  $D$  by the Stokes–Einstein equation:

$$D = k_B T / (6\pi\eta R_h)$$

where  $k_B$  is the Boltzmann constant,  $T$  is the absolute temperature, and  $\eta$  is the viscosity of the solvent.

### 2.3. SANS measurements

SANS measurements were performed in the Center for Neutron Research at the National Institute for Standards and Technology on the NG3 30m instrument with a neutron wavelength of  $\lambda = 6.0 \text{ \AA}$  ( $\Delta\lambda/\lambda \sim 0.15$ ). Two sample-detector distances were used (1.33 m and 8.00 m), which leads to an overall  $q$ -range of  $0.0042 < q = 4\pi\lambda^{-1} \sin \theta < 0.045 \text{ \AA}^{-1}$ , where  $2\theta$  is the angle of scatter. The data were corrected for instrumental backgrounds as well as detector efficiency and put on absolute scale [the cross-section  $I(q)$  in units of  $\text{cm}^{-1}$ ] based on direct beam flux method. Scattering from the solvent was subsequently subtracted [25]. The neutron cross-section was measured as a function of polymer concentration and temperature. It may be expressed as [26]:

$$I(q) = \frac{\phi(\Delta\rho)^2}{V_p} P(q)V_p^2 S'(q) + bkg \quad (1)$$

where  $P(q) = |F(q)|^2$  is the form factor,  $F(q)$  is the form factor amplitude,  $\phi$  is the volume fraction of the particles,  $\Delta\rho$  is the scattering length density difference between the particle and solvent ( $\text{D}_2\text{O}$ ,  $6.4 \times 10^{-6} \text{ \AA}^{-2}$ ),  $V_p$  is the volume of one particle and  $S(q)$  is the structure factor which can be modeled by the modified Ornstein–Zernike function [26b] which has been widely used to account for the attractive interactions near the phase boundary of various microemulsion systems [26c,d]:

$$S'(q) = 1 + \beta \frac{S(0)}{1 + (q\xi)^2}, \quad \text{where } \beta = \frac{\langle F(q) \rangle^2}{\langle |F(q)|^2 \rangle} \quad (2)$$

All solutions were prepared in  $\text{D}_2\text{O}$  and refrigerated at  $T = 15 \text{ }^\circ\text{C}$  (i.e. far below  $T_{\text{CP}}$ ) for several days before the experiments. The temperature range covered in the experiments was  $25\text{--}55 \text{ }^\circ\text{C}$  and the temperature was controlled to better than  $\pm 0.2 \text{ }^\circ\text{C}$  using a water circulation bath. Before starting the measurements, solutions were equilibrated at each temperature for 60–90 min, and this interval much exceeds the characteristic equilibration time of  $\sim 5 \text{ min}$  for  $1^\circ$  step determined using light scattering. The run times at each temperature at the 8.00 m sample-detector distance (SDD) were 10 min, 30 min and 80 min for 1.8 wt%, 0.3 wt% and 0.1 wt% solutions, respectively. At SDD = 1.33 m, the run time for all solutions was 5 min.

## 3. Results and discussion

### 3.1. Clusters and solubility

Fig. 2 represents the results of DLS measurements for two PTrEGS aqueous solutions (0.1 wt% with  $T_{\text{CP}} \sim 45 \text{ }^\circ\text{C}$  and 1.8 wt% with  $T_{\text{CP}} \sim 40 \text{ }^\circ\text{C}$ ) at different temperatures. The results clearly indicate the existence of two populations of the polymer species in solutions below their  $T_{\text{CP}}$ s. The smaller species are individual polymers characterized by a relatively narrow size distribution with dimensions (40–50  $\text{\AA}$ ) that are similar in both solutions. The larger species are identified as polymer clusters (aggregates) with a broad size distribution in the range of 400–1000  $\text{\AA}$  for 0.1 wt% and 1000–10000  $\text{\AA}$  for 1.8 wt% solutions. Clustering phenomena in PEG/water system have attracted considerable attention and various mechanisms, such as impurities, crystallization, hydrogen bonding, hydrophobic backbone, and end group interactions have been proposed [28]. Comparison of the areas under the corresponding peaks shows that the amount of individual polymers in solution is small ( $\sim 2\text{--}3 \text{ wt\%}$ ). As the temperature increases and approaches  $T_{\text{CP}}$ , the clusters in both solutions grow in size due to association. The size distribution of cluster in the 0.1 wt% solution narrows and its average size becomes smaller at temperatures above  $T_{\text{CP}}$  ( $45 \text{ }^\circ\text{C}$ ). The same

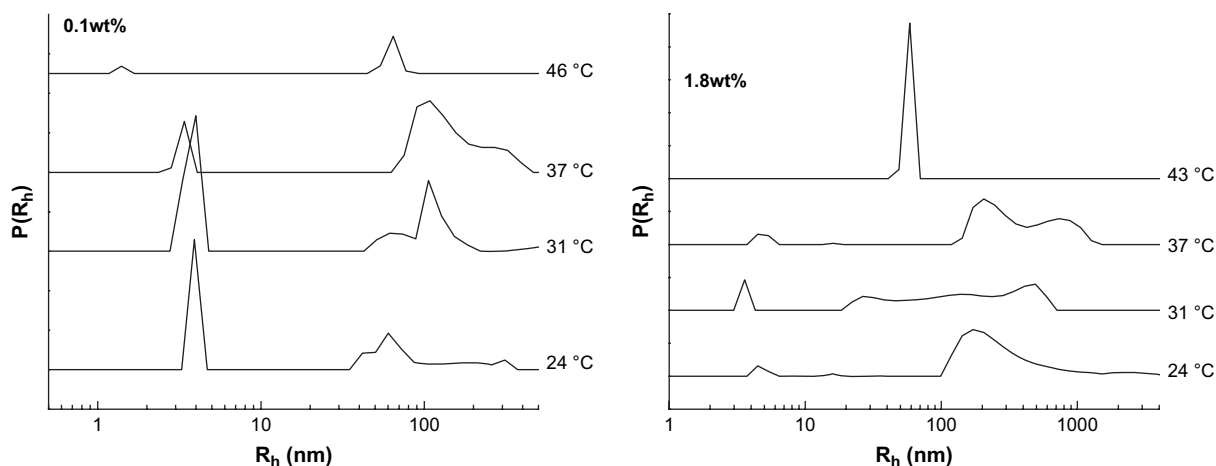


Fig. 2. Hydrodynamic radius distribution as a function of temperature for 0.1 wt% and 1.8 wt% PTrEGS solutions in  $\text{D}_2\text{O}$ .

effect is observed for the 1.8 wt% solution (40 °C), where the size of the remaining clusters in solution decreases significantly and becomes comparable to the size of the clusters above  $T_{CP}$  of the 0.1 wt% solution ( $\sim 700$ – $800$  Å). As will be discussed below, the observed decrease of the cluster sizes is due to the precipitation of a fraction of large clusters above  $T_{CP}$  and/or dehydration of the clusters.

Neutron transmission is defined as the ratio of the transmitted beam intensity after attenuation by the sample to the incident neutron intensity. It is one of the parameters used for converting the intensity of scattering in counts per second into neutron cross-section with unit of  $\text{cm}^{-1}$ . Due to the fact that the total neutron cross-section of hydrogen is much higher than the cross-sections of other atoms, the transmission is highly sensitive to the presence of protonated materials in the beam [27]. Thus, transmission measurements provide information on the concentration of the protonated polymer in the deuterated solvent. When any polymer precipitates to the bottom of the cell at a given temperature, it does not contribute to the attenuation, since the beam diameter (1.2 cm) is smaller than that of the cell (2 cm). As shown in Fig. 3, the transmission of the 1.8 wt% solution increases between 38 °C and 43 °C. This indicates that a fraction of the largest polymer clusters precipitates from the solution in this temperature range, which resulted in a decrease of average size of the clusters still remaining in the solution. At the same time, the solution transmission remains constant above 43 °C and thus a fraction of smaller clusters and individual polymers remains dissolved in  $\text{D}_2\text{O}$  up to a temperature of 55 °C. As will be discussed later, the SANS data suggest the presence of smaller compact clusters (due to dehydration) in the solutions at 55 °C. The transmission of dilute solutions, 0.1 wt% and 0.3 wt% solutions, remains constant within experimental error both below and above the corresponding  $T_{CPs}$  (Fig. 3). However, precipitation of some large clusters above  $T_{CP}$  cannot be ruled out in these systems because of the low concentration of the polymer in solution; which makes it difficult to detect the changes in the transmission due to the small amount of polymer precipitation.

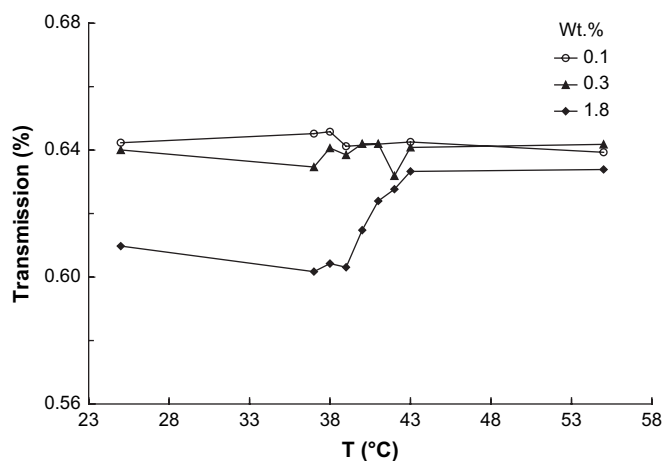


Fig. 3. Neutron transmission of the studied solutions as a function of temperature.

### 3.2. Structure of individual PTrEGS polymers in toluene-*d*

Toluene is a good solvent for both the backbone (PS) and the side group (EG) and thus it is considered as a solvent of choice for measuring the form factor of individual (non-interacting) polymers. SANS data for the 1.8 wt% solution of the polymers in toluene-*d* are shown in Fig. 4. The assumption that SANS from this solution arises from individual polymer chains was confirmed by comparing the measured and calculated values of the zero angle neutron cross-section  $I(0) = \phi \Delta \rho^2 V_p$  as obtained from Eq. (1) taking into account that  $P(q=0) = S(q=0) = 1$ . For 1.8 wt% polymers in toluene-*d*, using  $\Delta \rho = 4.76 \times 10^{-6} \text{ \AA}^{-2}$  and  $V_p = 14\,300 \text{ \AA}^3$ , the calculated  $I(0) \sim 0.050 \text{ cm}^{-1}$  which agrees well with experimental value of  $I(0) \sim 0.063 \text{ cm}^{-1}$ . This further confirmed that the SANS data for the 1.8 wt% of PTrEGS polymer in toluene-*d* were from single chain scattering.

Comb-like polymers can adopt a variety of shapes depending on the ratio between the length of the backbone and side chain polymers [29]. When the size of the backbone is smaller than that of the side chains, the polymer tends to adopt a spherical conformation. As the length of the backbone increases, ellipsoidal or cylindrical conformation becomes more favorable [29c]. Therefore we expect that the shape of the polymer in a homogeneous domain below  $T_{CP}$  is either a prolate ellipsoid or a short cylinder. By fitting the data to each of the form factors we obtained  $R_a = 37 \text{ \AA}$ ,  $R_b = 14 \text{ \AA}$  for the ellipsoidal model and  $R_a = 14 \text{ \AA}$ ,  $R_b = 54 \text{ \AA}$  for the cylindrical model (see Fig. 4). The quality of fits as well as the values of calculated volumes of the ellipsoid and cylinder is similar and the SANS results do not allow for favoring one model over the other.

### 3.3. Structure and interactions in PTrEGS- $\text{D}_2\text{O}$ solutions

Unlike toluene, water is a non-solvent for the backbone of the studied polymer and thus strong association/clustering effects may be anticipated in aqueous solutions of PTrEGS because of the poorer overall solvent quality. SANS data for

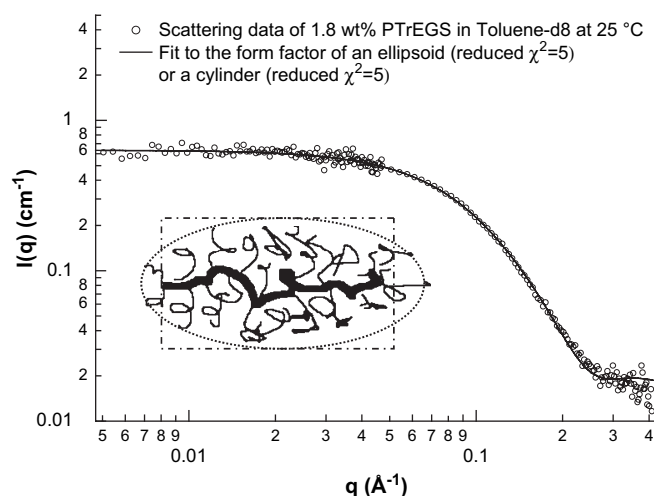


Fig. 4. SANS data of 1.8 wt% PTrEGS in  $\text{D}_2\text{O}$  and toluene-*d* at 25 °C.

0.1 wt%, 0.3 wt% and 1.8 wt% solutions in the temperature range 25–55 °C are shown in Fig. 5. The upturn at small values of scattering vectors at  $T < T_{CP}$  represents a “tail” of

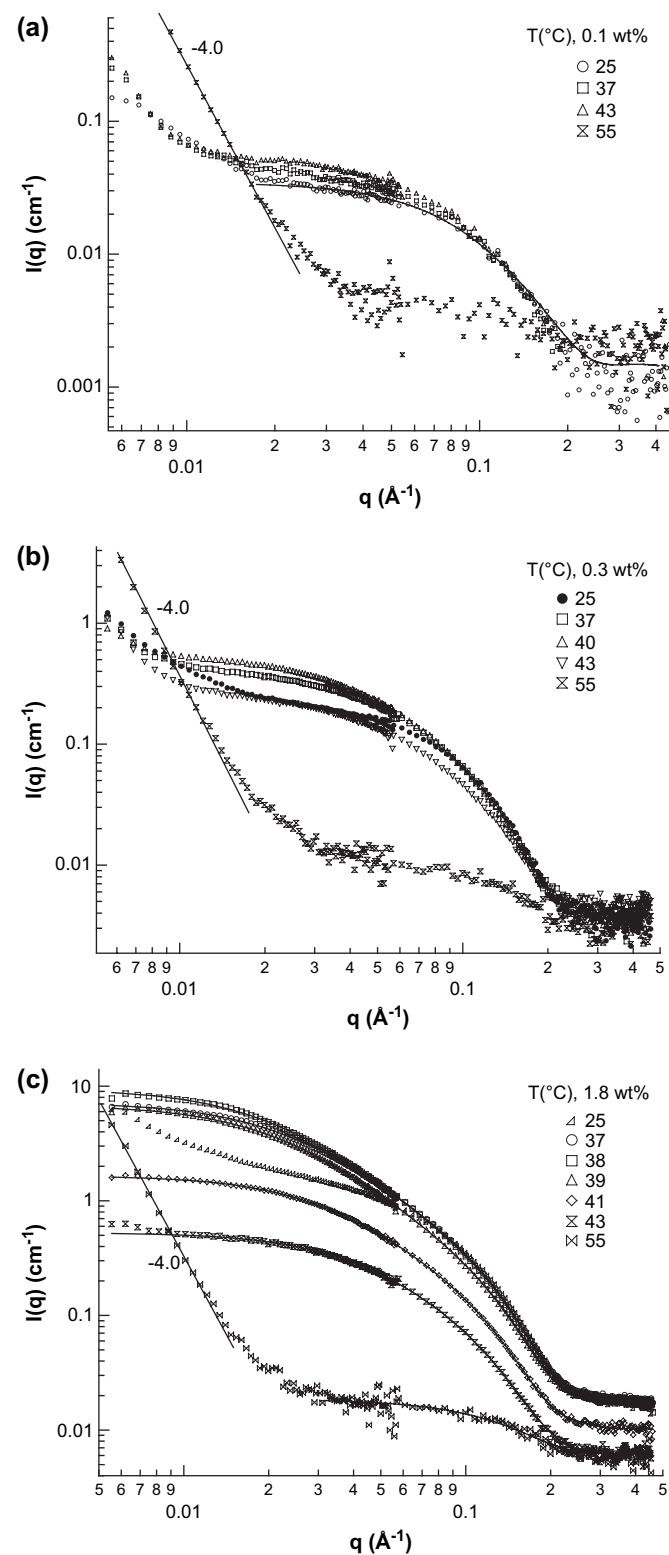


Fig. 5. SANS data of the (a) 0.1 wt% and (b) 0.3 wt% and (c) 1.8 wt% solution at different temperatures. The solid lines are fits to the models described in the text. The error bars on the SANS curves are removed for the sake of clarification.

the scattering function from large and relatively loose clusters, the size of which is too big to be resolved using SANS. The value of the scattering vector ( $q^*$ ) at which the upturn starts to appear is concentration dependent:  $q^* = 0.06 \text{ \AA}^{-1}$  for 0.1 wt% solution,  $q^* = 0.008 \text{ \AA}^{-1}$  for 0.3 wt% solution and 1.8 wt% solution.

Fitting the SANS data for the dilute aqueous solution (0.1 wt%) at temperature ( $T = 25 \text{ °C}$ ) well-below the corresponding cloud point ( $T_{CP} = 45 \text{ °C}$ ) gives  $R_a = 36 \text{ \AA}$ ,  $R_b = 16 \text{ \AA}$  for the ellipsoidal model and  $R_a = 15 \text{ \AA}$ ,  $R_b = 52 \text{ \AA}$  for the cylindrical model. Within experimental error, these results agreed well with the data obtained from solutions of PTrEGS in toluene-*d*. This result is surprising because of significant difference in the solvent quality with respect to the backbone polymer. We speculate that the dimension of PTrEGS chains in  $D_2O$  remains similar to that in toluene-*d* because the solvation of the side chains screens out backbone–solvent interactions and prevents chain contraction at  $T < T_{CP}$ . This assumption is supported by the globularisation of the PTrEGS chains above  $T_{CP}$  due to almost complete dehydration of the side chains of the polymer (see below).

The scattering intensity in the “intermediate range” increases with temperature and reaches a maximum at  $T = T_{CP}$  of each solution. The increase of  $I(q)$  as  $T \Rightarrow T_{CP}$  is due to the polymer–polymer attractive interactions. This interaction becomes stronger as the phase boundary is approached [26]. Moreover, solution concentration plays a critical role in the interaction. For example, the probability of the polymer–polymer interactions in very dilute solutions can be negligible. Thus it is reasonable that there is only a minor increase in  $I(q)$  in the  $q > q^*$  domain from  $\sim 0.03$  to  $\sim 0.06 \text{ \AA}^{-1}$  for 0.1 wt% and 0.3 wt% solutions, respectively (see Fig. 5a and b). In addition, the scattering curves for these solutions can be fitted to Eq. (1) (O–Z equation) to extract the form factor only ( $S(q)$  in Eq. (1)  $\approx 1$  for weakly interacting chains). The situation is different for the more concentrated solution (1.8 wt%), where the interactions between polymers become strong enough to make a significant contribution to the structure factor. Fitting of the SANS data to the model of ellipsoids with attractive interactions at different temperatures below  $T_{CP}$  gives the fitting parameters shown in Table 1. The results demonstrate that the

Table 1

Results from fitting the 1.8 wt% SANS data to an ellipsoid form factor with an Ornstein–Zernike structure factor

$T$ (°C)	$R_a$ (Å)	$R_b$ (Å)	$\xi$ (Å)	$S(0)$
37	31	15	42	13
38(CP)	29	15	49	22
39	30	15	45	20
40	29	15	37	15
41	31	15	30	8
42	30	15	27	6
43	28	15	24	4

$R_a$  is the rotation axis and  $R_b$  is the short axis of an ellipsoid.  $\xi$  stands for the interaction distance and  $S(0)$  is related to the interaction strength. The errors generated from the fitting are less than 1.0 for these four parameters and are not included in this table.

dimensions of the individual polymers remain unchanged in the vicinity of the cloud point. On the other hand, the characteristic distance (correlation length  $\xi$ ) as well as the amplitude, or susceptibility of the interactions, which is proportional to  $S(0)$ , changes significantly and reaches maximum values near  $T_{CP}$  ( $\xi \sim 49$  and  $S(0) \sim 22$ ).

At temperatures *far above* the  $T_{CP}$  of each solution ( $T = 55$  °C), the scattering pattern changes dramatically. The total neutron cross-section decreases because of the precipitation of some of the polymer above  $T_{CB}$  as discussed above. In the low  $q$  limit compact clusters with sharp interfaces are formed as evidenced by SANS with an exponent ( $n$ ) of  $-4.0$  ( $I(q) \sim q^n$ ) for  $q < 0.015 \text{ \AA}^{-1}$ . SANS data from 1.8 wt% solutions in the  $q > q^*$  region (see Fig. 5c) can be fitted to a form factor of a mostly dehydrated spherical globules with a radius of  $15 \text{ \AA}$ . The globules remain dissolved and do not precipitate, probably due to the availability of water-soluble EG chains in the outer shell of the globule [20a]. The statistics of the high- $q$  data for most dilute solutions of 0.1 wt% and 0.3 wt% is not sufficient to provide reliable fits to the spherical model in the  $q > q^*$  domain.

In summary, the conformation and interactions between PTrEGS polymers in aqueous solutions have been studied by SANS and DLS. The polymer conformation was confirmed by the SANS data for 1.8 wt% polymer solution in toluene- $d$ , which provided the form factor of the polymers in  $D_2O$ . It was found that the individual polymers adopt ellipsoidal or short cylindrical shapes in both toluene- $d$  and  $D_2O$  at  $T \ll T_{CP}$ . The individual polymers coexist with loose clusters even in dilute aqueous solution (0.1 wt%) at 25 °C. With increasing temperature, up to  $T_{CP}$ , clusters become larger while interactions between polymers become stronger. At higher polymer concentrations, the interactions can be described by the O–Z equation around the  $T_{CP}$ . The polymer dimensions remain approximately constant at  $T \leq T_{CP}$  while the interactions are temperature dependent and reach maximum around  $T_{CP}$ . At temperatures  $\sim 15$  °C above  $T_{CP}$ , polymers collapse into a spherical globules with the diameter  $\sim 15 \text{ \AA}$ .

## Acknowledgements

Research sponsored by the Division of Materials Sciences and Engineering, Office of Basic Energy Sciences, U.S. Department of Energy, under contract DE-AC05-00OR22725 with Oak Ridge National Laboratory, managed and operated by UT-Battelle, LLC. Part of this research was conducted at the Center for Nanophase Materials Sciences, which is sponsored at ORNL by the Division of Scientific User Facilities, U.S. Department of Energy. We acknowledge the support of the National Institute of Standards and Technology, U.S. Department of Commerce, in providing the neutron research facilities used in this work. G. Cheng and F. Hua are supported in part by an appointment to the ORNL Postdoctoral Research Associates Program, administered jointly by the ORNL and the Oak Ridge Associated Universities.

## References

- [1] de las Heras Alarcon C, Pennadam S, Alexander C. *Chem Soc Rev* 2005; 34:276.
- [2] Saitoh T, Sekino A, Hiraide M. *Chem Lett* 2004;33:912.
- [3] Bergbreiter DE. *Chem Rev* 2002;102:3345.
- [4] Fujii S, Read ES, Binks RP, Armes SP. *Adv Mater* 2005;17:1014.
- [5] Wu C, Qiu X. *Phys Rev Lett* 1998;80:620.
- [6] Wu C, Wang X. *Phys Rev Lett* 1998;80:4092.
- [7] Saunders BR. *Langmuir* 2004;20:3925.
- [8] Ono Y, Shikata T. *J Am Chem Soc* 2006;128:10030.
- [9] (a) Cheng H, Wu C. *Macromolecules* 2006;39:2325; (b) Kujawa P, Aseyev V, Tenhu H, Winnik FM. *Macromolecules* 2006; 39:7686 and references therein.
- [10] Feng X, Taton D, Borsali R, Chaikof EL, Gnanou Y. *J Am Chem Soc* 2006;128:11551 and references therein.
- [11] Liu G, Reinhout M, Mainguy B, Baker GL. *Macromolecules* 2006;39: 4726.
- [12] Jannasch P, Hassander H, Wesslen B. *J Polym Sci Part B Polym Phys* 1996;34:1289.
- [13] Hallensleben ML, Lucarelli F. *Polym Bull* 1996;37:759.
- [14] Chang CJ, Kao PC. *Polymer* 2006;47:591.
- [15] Hyun J, Chen J, Setton LA, Chilkoti A. *Biomaterials* 2006;27:1444.
- [16] Kawaguchi S, Ito K. *Colloids Surf A Physicochem Eng Aspects* 1999;153: 173.
- [17] Connolly R, Bellesia G, Timoshenko EG, Kuznetsov YA, Elli S, Ganazzoli F. *Macromolecules* 2005;38:5288.
- [18] (a) Amitani K, Terao K, Nakamura Y, Norisuye T. *Polym J* 2005;37:324; (b) Zhao Y, Jamieson AM, Olson BG, Yao N, Dong S, Nazarenko S, et al. *J Polym Sci Part B Polym Phys* 2006;42:2412; (c) Rathgeber S, Pakula T, Wilk A, Matyjaszewski K, Beers KL. *J Chem Phys* 2005;122:124904.
- [19] (a) Sheng YJ, Cheng KL, Ho CC. *J Chem Phys* 2004;121:1962; (b) Fisher K, Schmidt M. *Macromol Rapid Commun* 2001;22:787.
- [20] (a) Qiu X, Wu C. *Macromolecules* 1997;30:7921; (b) Virtanen J, Tenhu H. *Macromolecules* 2000;33:5970.
- [21] (a) Crower HM, Saunders BR, Mears SJ, Cosgrove T, Vincent B, King SM, et al. *Colloids Surf A Physicochem Eng Aspects* 1999;152:327; (b) Kratz K, Hellweg T, Eimer W. *Polymer* 2001;42:6631; (c) Stieger M, Richtering W, Pedersen JS, Lindner P. *J Chem Phys* 2004; 120:6197; (d) Arleth L, Xia X, Hjelm RP, Wu J, Hu Z. *J Polym Sci Part B Polym Phys* 2005;43:849.
- [22] (a) Shibayama M, Isono K, Okabe S, Karino T, Nagao M. *Macromolecules* 2004;37:2909; (b) Rehfeldt F, Steitz R, Armes SP, von Klitzing R, Gast A, Tanaka MJ. *Phys Chem B* 2006;110:9177.
- [23] (a) Hua F, Jiang X, Zhao B. *Macromolecules* 2006;39:3476; (b) Zhao B, Li DJ, Hua F. *Macromolecules* 2005;38:9509.
- [24] Wignall GD. In: Mark JE, editor. *Physical properties of polymers*. 3rd ed. New York: Cambridge University Press; 2004. p. 424–511 [chapter 7].
- [25] Dubner WS, Schultz JM, Wignall GD. *J Appl Crystallogr* 1990;23:469.
- [26] (a) Guinier A, Fournet G. *Small-angle scattering of X-rays*. New York: John Wiley and Sons; 1955; (b) Kotlarchyk M, Chen S-H. *J Chem Phys* 1983;79:2461; (c) Steytler D, Rumsey E, Thorpe M. *Langmuir* 2001;17:7948; (d) Xu B, Lynn GW, Guo J, Melnichenko YB, Wignall GW, McClain JB, et al. *J Phys Chem B* 2005;109:10261.
- [27] (a) Melnichenko YB, Klepko V, Shilov V. *Polymer* 1988;29:1010; (b) Melnichenko YB, Wignall GD, Compton RN, Bakale G. *J Chem Phys* 1999;111:4724.
- [28] Hammouda B, Ho DL, Kline S. *Macromolecules* 2004;37:6932.
- [29] (a) Desvergne S, Heroguez V, Gnanou Y, Borsali R. *Macromolecules* 2005;38:2400; (b) Wataoka I, Urakawa H, Kajiwara K, Schmidt M, Wintermantel M. *Polym Int* 1997;44:365; (c) Denesyuk NA. *Phys Rev E* 2003;68:031803.